Mineralogical Magazine, December 2018, Vol. 82(6), pp. 1323–1332

Beusite-(Ca), ideally $CaMn_2^{2+}(PO_4)_2$, a new graftonite-group mineral from the Yellowknife pegmatite field, Northwest Territories, Canada: Description and crystal structure

Frank C. Hawthorne[1,*], Michael A. Wise[2], Petr Černý[1], Yassir A. Abdu[3], Neil A. Ball[1], Adam Pieczka[4] and Adam Włodek[4]

[1] Department of Geological Sciences, University of Manitoba, Winnipeg, Manitoba R3T 2N2, Canada
[2] Department of Mineral Sciences, Smithsonian Institution, PO Box 37012, MRC 119, Washington, DC 0013-7012
[3] Department of Applied Physics and Astronomy, University of Sharjah, P.O. Box 27272, Sharjah, United Arab Emirates
[4] AGH University of Science and Technology, Department of Mineralogy, Petrography and Geochemistry, 30-059 Kraków, Mickiewicza 30, Poland

[*Received 26 November 2017; Accepted 6 March 2018; Associate Editor: Anthony Kampf*]

ABSTRACT

Beusite-(Ca), ideally $CaMn_2^{2+}(PO_4)_2$, is a new graftonite-group mineral from the Yellowknife pegmatite field, Northwest Territories, Canada. It occurs in a beryl–columbite–phosphate rare-element pegmatite where it is commonly intergrown with triphylite–lithiophilite or sarcopside, and may form by exsolution from a high-temperature (Li,Ca)-rich graftonite-like parent phase. It occurs as pale-brown lamellae 0.1–1.5 mm wide in triphylite, and is pale brown with a vitreous lustre and a very pale-brown streak. It is brittle, has a Mohs hardness of 5, and the calculated density is 3.610 g/cm^3. Beusite-(Ca) is colourless in plane-polarized light, and is biaxial (+) with $\alpha = 1.685(2)$, $\beta = 1.688(2)$, $\gamma = 1.700(5)$, and the optic axial angle is 46.0(5)°. It is non-pleochroic with $X \parallel b$; $Y \wedge a = 40.3°$ in β obtuse; $Z \wedge a = 49.7°$ in β acute. Beusite-(Ca) is monoclinic, has space group $P2_1/c$, $a = 8.799(2)$, $b = 11.724(2)$, $c = 6.170(1)$ Å, $\beta = 99.23(3)°$, $V = 628.3(1)$ Å^3 and $Z = 4$. Chemical analysis by electron microprobe gave P_2O_5 41.63, FeO 19.43, MnO 23.63, CaO 15.45, sum 100.14 wt.%. The empirical formula was normalized on the basis of 8 anions pfu: $(Ca_{0.94}Fe_{0.92}Mn_{1.13})_{\Sigma 2.99}(PO_4)_{2.00}$. The crystal structure was refined to an R_1 index of 1.55%. Beusite-(Ca) is a member of the graftonite group with Ca completely ordered at the [8]-coordinated $M(1)$ site.

Keywords: beusite-(Ca), new mineral, chemical analysis, crystal structure, Raman spectrum, Yellowknife pegmatite field, Northwest Territories, Canada.

Introduction

Graftonite and beusite are common late-stage accessory minerals in complex granitic pegmatites (e.g. Fransolet *et al.*, 1986; Černý *et al.*, 1998; Smeds *et al.*, 1998; Pieczka, 2007; Guastoni *et al.*, 2007; Vignola *et al.*, 2008; Galliski *et al.*, 2009; Ercit *et al.*, 2010). They have also been found as constituents of phosphate-oxide inclusions in IIIAB iron meteorites (Bild, 1974; Steele *et al.*, 1991; Olsen *et al.*, 1999), and Stalder and Rozendaal (2002) reported graftonite as a primary phase in a phosphorous-rich iron formation. Penfield (1900) described graftonite, ideally $[Fe_3^{2+}(PO_4)_2]$, from a granitic pegmatite in New Hampshire. Beus (1950) reported a graftonite-like mineral with Mn^{2+} dominant over Fe^{2+}, and Hurlbut and Aristarain (1968) described beusite, ideally $[Mn_3^{2+}(PO_4)_2]$, as a distinct species from the pegmatites of the San Luis province, Argentina. The crystal structures of graftonite and beusite were solved by Calvo (1968) and Hurlbut and

*E-mail: frank_hawthorne@umanitoba.ca
https://doi.org/10.1180/mgm.2018.120

Aristarain (1968), and Steele *et al.* (1991) and Wise *et al.* (1990) refined the structures of Ca-free and Ca-rich beusite, respectively. The structure of graftonite–beusite is a dense framework of polyhedra (Hawthorne, 1998; Huminicki and Hawthorne, 2002), and Tait *et al.* (2013) concluded that the coordination numbers of the sites occupied by Fe^{2+}, Mn^{2+} and Ca^{2+} (and minor Mg^{2+}) are as follows: $M(1) = [8]$, $M(2) = [5]$, $M(3) = [6]$. As a result, there is very strong order of cations over the $M(1)$, $M(2)$ and $M(3)$ sites, and Hawthorne and Pieczka (2018) have introduced a new nomenclature and classification scheme for these minerals.

Beusite-(Ca), $CaMn_2(PO_4)_2$, is a Ca analogue of beusite with Ca^{2+} completely ordered at the $M(1)$ site. The name is in accord with the nomenclature scheme for the graftonite group approved by the International Mineralogical Association Commission on New Minerals, Nomenclature and Classification (memorandum 66–SM/17 Hålenius *et al.* (2017)). The holotype sample is deposited in the mineral collection of the Department of Mineral Sciences, National Museum of Natural History, Smithsonian Institution, Washington, D.C., 20560, USA, catalogue number 177054.

Occurrence

Beusite-(Ca) occurs in a small pegmatite dyke in the regionally zoned Peg swarm of the Archean Yellowknife pegmatite field, and is located between Upper Ross Lake and Redout Lake, 75 km northeast of Yellowknife and 3.5 km east of the Redout granite, Canada (62°44′37″N, 113°6′26″W, Wise and Černý, 1990). The pegmatite is lenticular, strikes N–S, dips 45–70°E and cuts an interlayered sequence of amphibolite and granodiorite. The pegmatite is of the beryl–columbite–phosphate subtype of rare-element pegmatites (Černý, 1989) and shows well-developed, although not continuous, internal zonation; much of the primary zonation is obscured by albite units. The border zone is a fine-grained muscovite + quartz assemblage, followed by a fine-grained microcline perthite + quartz + muscovite + 'cleavelandite' wall-zone. Most of the pegmatite is composed of a coarse-grained microcline perthite (graphic) + quartz + muscovite + 'cleavelandite' + beryl zone that hosts most of the accessory minerals. The core is discontinuous and consists of coarse-grained quartz-microcline + accessory beryl.

Accessory minerals include 'biotite', yellow-green beryl, columbite-(Fe)–tantalite-(Fe), tapiolite-(Fe), almandine and pyrite.

Physical properties

Beusite-(Ca) forms pale-brown lamellae 0.1–1.5 mm wide, intergrown with triphylite lamellae (Fig. 1*a*); associated beusite-(Ca) lamellae are in optical orientation with each other. The beusite–triphylite intergrowths occur as a 6 cm × 5 cm × 3 cm nodule (Fig. 1*b*). Beusite-(Ca) is pale brown and

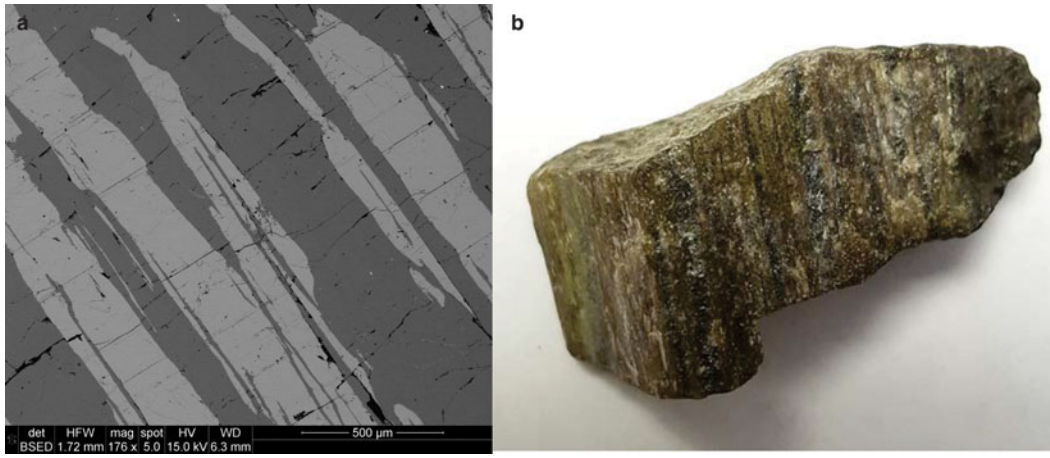

FIG. 1. (*a*) Back-scatter electron image showing intergrowths of beusite (light) and triphylite (dark); (*b*) the nodule (6 cm × 5 cm × 3 cm) in which beusite-(Ca) was discovered.

https://doi.org/10.1180/mgm.2018.120 Published online by Cambridge University Press

TABLE 1. Chemical composition (wt.%) of beusite-(Ca).

Constituent	Mean	Range
P_2O_5	41.63(47)	41.00–42.10
FeO	19.43(44)	19.00–19.80
MnO	23.63(98)	23.10–25.10
MgO	nd	
CaO	15.45(81)	14.30–16.10
Total	100.14	

nd – not detected.

transparent with a vitreous lustre and a very pale-brown streak; it does not fluoresce in either longwave or shortwave ultraviolet light. It is brittle with an irregular fracture, and has a Mohs hardness of 5. Cleavage is good on both {010} and {100}, there is no parting, and the calculated density is 3.610 g/cm^3. To measure the optical properties, a crystal was mounted on a Bloss spindle stage and the extinction curves were measured using white light. The resulting measurements were processed using Excalibr II (Bartelmehs *et al.*, 1992) and the 2V angle was derived. Excalibr II also provided the setting angles for measurement of refractive indices: $\alpha = 1.685(2)$, $\beta = 1.688(2)$, $\gamma = 1.700(5)$, α; $2V_{obs} = 46.0(5)°$, $2V_{calc} = 53°$; the dispersion is $r < v$, weak. No pleochroism was observed, small crystals (<50 μm) are colourless. The optic orientation was measured by transferring the crystal and goniometer head from the spindle stage to a single-crystal diffractometer and orienting the crystallographic axes: X ∥ *b*; Y ∧ *a* = 40.3° in β obtuse; Z ∧ *a* = 49.7° in β acute.

Chemical composition

Crystals were analysed with a Cameca SX100 electron microprobe operated in wavelength-dispersive mode at 15 kV and 20 nA, using a beam diameter of 2 μm. The following standards were used: apatite (P and Ca), chromite (Fe and Mg) and MnF_2 (Mn). The concentration of Mg was below the detection limit. Data reduction was done using the φ(ρZ) procedure of Pouchou and Pichoir (1985). Table 1 gives the chemical composition (mean of ten points). The empirical formula unit, calculated on the basis of 8 anions per formula unit, is $(Ca_{0.94}Mn_{1.14}Fe_{0.92})_{\Sigma 3.00}(PO_4)_{2.00}$, ideally $CaMn_2(PO_4)_2$.

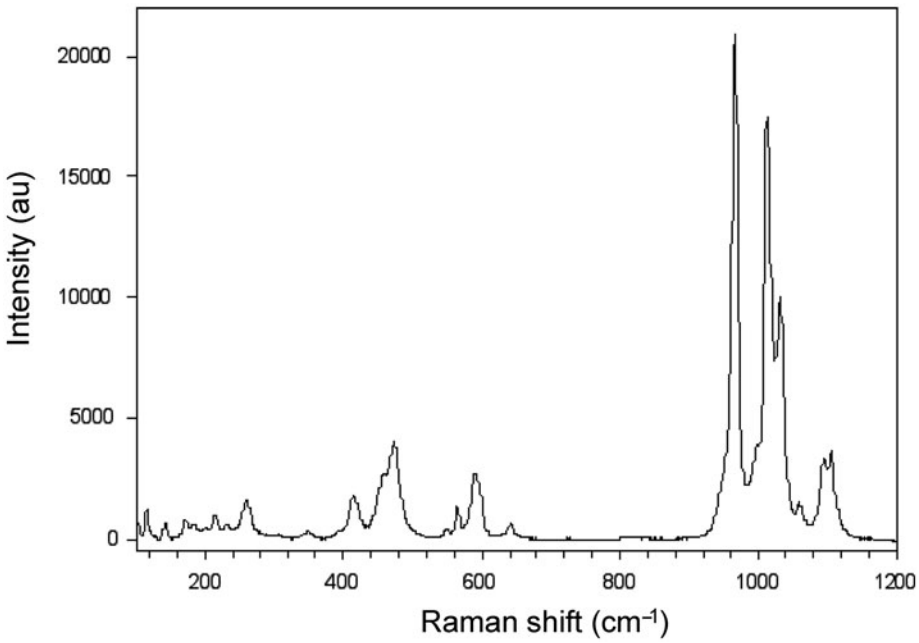

FIG. 2. The Raman spectrum of holotype beusite-(Ca).

https://doi.org/10.1180/mgm.2018.120 Published online by Cambridge University Press

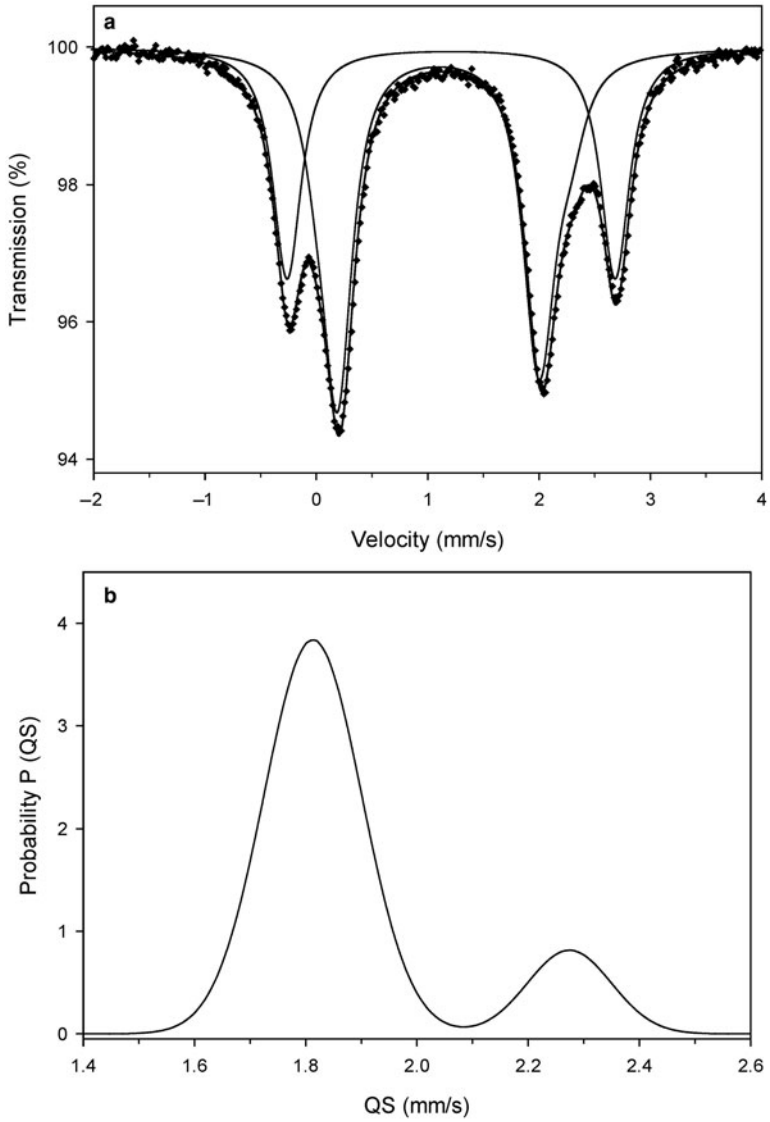

FIG. 3. The Mössbauer spectrum of a mixture of holotype beusite-(Ca) and triphylite., see text for details

Raman spectroscopy

The Raman spectrum of beusite-(Ca) was collected in back-scattered mode with a HORIBA Jobin Yvon-LabRAM ARAMIS integrated confocal micro-Raman system equipped with a 460 mm focal-length spectrograph and a multichannel air-cooled (–70°C) CCD detector. A magnification of 100× was used with an estimated spot size of 1 μm, a 1800 gr/mm grating, an excitation radiation of 532 nm, and laser power between 5 and 12.5 mW. Calibration was done using the 520.7 cm^{-1} line of Si metal, data were collected over the range 100–1200 cm^{-1} for 20 s, and the final spectrum is the average of two scans. In the Raman spectrum (Fig. 2), the peaks at 961, 1008 and 1027 cm^{-1} (strong), 1054 (w = weak) and 1090 and 1104 cm^{-1} (m = medium) may be assigned to stretching vibrations of the PO_4 groups. The peaks at 592 (vw = very weak), 562 (m), 548 (w), 473 (vw), 458 (w) and 416 (w)

https://doi.org/10.1180/mgm.2018.120 Published online by Cambridge University Press

TABLE 2. Mössbauer parameters for beusite-(Ca)–triphylite mixture.

Assignment	CS (mm/s)	QS (mm/s)	Rel. Area (±2 %)
Fe^{2+} [beusite-(Ca)-M2]	1.12	1.81	54
Fe^{2+} [beusite-(Ca)-M3]	1.18	2.27	9
Fe^{2+} (triphylite)	1.23	2.95	37

CS – centre shift; QS – quadropole splitting.

cm^{-1} are due to the bending vibrations of PO_4 and stretching vibrations of CaO_8 and MnO_6 polyhedra. The peaks at 347 (vw), 261 (w), 231 (vw), 212 (w), 182 (vw), 160 (vw), 140 (vw) and 115 (vw) cm^{-1} are due to angular deformations of the CaO_8 and MnO_6 polyhedra.

Mössbauer spectroscopy

Mössbauer spectroscopy was done in transmission geometry at room temperature (RT) using a ^{57}Co

TABLE 3. X-ray powder diffraction pattern for beusite-(Ca).

I	*d*(Å)	*h*	*k*	*l*	*I*	*d*(Å)	*h*	*k*	*l*
5	6.979	1	1	0	15	1.918	4	0	2
6	4.913	1	1	1		–	3	1	2
18	4.321	$\bar{1}$	1	1					
8	4.224	0	2	1	17	1.894	4	3	0
13	3.648	$\bar{2}$	1	1					
97	**3.564**	**1**	**3**	**0**	17	1.889	$\bar{4}$	3	1
8	3.170	$\bar{1}$	3	1		–	3	4	1
	–	2	1	1	22	1.893	0	6	1
58	**3.030**	**$\bar{1}$**	**0**	**2**		–	$\bar{2}$	2	3
76	**2.991**	**1**	**3**	**1**	12	1.816	$\bar{1}$	3	3
87	**2.932**	**0**	**4**	**0**		–	1	2	3
	–	$\bar{1}$	1	2	12	1.801	$\bar{3}$	4	2
100	**2.904**	2	3	0		–	0	3	3
86	**2.873**	**2**	**2**	**1**					
11	2.811	3	1	0	21	1.782	2	6	0
16	2.777	1	4	0		–	1	5	2
86	**2.718**	**$\bar{3}$**	**1**	**1**	21	1.772	$\bar{2}$	5	2
17	2.668	1	1	2	17	1.743	4	3	1
10	2.637	$\bar{2}$	1	2		–	3	3	2
6	2.577	$\bar{1}$	4	1	20	1.738	$\bar{4}$	4	1
11	2.522	$\bar{3}$	2	1		–	5	0	0
7	2.480	1	4	1	22	1.717	5	1	0
	–	1	1	2		–	2	1	3
37	2.413	3	1	1	13	1.699	3	5	1
16	2.327	$\bar{2}$	4	1	15	1.665	0	4	3
	–	3	3	0		–	5	2	0
10	2.274	2	1	2		–	2	2	3
	–	$\bar{3}$	3	1	13	1.645	4	0	2
8	2.161	2	2	2		–	1	7	0
12	2.135	$\bar{3}$	2	2		–	0	6	2
	–	4	1	0	8	1.631	$\bar{2}$	4	3
16	2.094	1	5	1		–	4	1	2
18	2.061	2	5	0	12	1.623	4	4	1
	–	3	4	0	11	1.602	$\bar{1}$	7	1
18	2.001	$\bar{2}$	5	1	8	1.563	$\bar{5}$	2	2
	–	1	4	2		–	2	7	0
22	1.975	$\bar{3}$	3	2	13	1.544	5	2	1
47	**1.937**	**$\bar{2}$**	**1**	**3**			$\bar{1}$	5	3
	–	$\bar{1}$	2	3			$\bar{1}$	0	4

https://doi.org/10.1180/mgm.2018.120 Published online by Cambridge University Press

TABLE 4. Miscellaneous information for beusite-(Ca).

Crystal data	
Crystal size (μm)	30 × 30 × 60
Space group	$P2_1/c$
a (Å)	8.7990(18)
b	11.724(2)
c	6.1700(12)
β (°)	99,23(3)
V (Å^3)	628.3(8)
Z	4
Data collection	
Radiation	Mo$K\alpha$
No. of reflections	22,619
No. in Ewald sphere	4083
No. unique reflections	1852
No. with ($F_o > 4\sigma F$)	1832
Structure refinement	
Variable parameters	122
GoF	1.037
R_{int}%	1.25
R_1%	1.55
wR_2%	4.25
Cell content:	4 [$CaMn_2^{2+}(PO_4)_2$]

$R_1 = \Sigma(|F_o| - |F_c|) / \Sigma|F_o|$; $wR_2 = [\Sigma w (F_o^2 - F_c^2)^2 / \Sigma w (F_o^2)^2]^{½}$, $w = 1/[\sigma^2(F_o^2) + (0.0241P)^2 + 0.53P]$ where $P = (\text{Max}(F_o^2,0) + 2F_c^2)/3$

(Rh) point source. For preparing the Mössbauer absorber, the powdered sample of beusite-(Ca) was mixed with sugar and loaded into a Pb disk with 5 mm inner diameter. The spectrum was analysed in terms of a Voigt-function-based quadrupole-splitting distribution (QSD) (Rancourt and Ping, 1991) using the RECOIL® software package. The centre shift (CS) is given relative to α-Fe at RT. The Mössbauer spectrum of beusite-(Ca) is shown in Fig. 3. It was fitted to a QSD model having two generalized QSD sites, one for Fe^{2+} in beusite-(Ca) (with two Gaussian components) and the other for Fe^{2+} in triphylite (with one Gaussian component) (Fig. 3*a*). The Mössbauer parameters are given in Table 2. The QSD curve for Fe^{2+} in beusite-(Ca) shows two well-resolved Gaussian components centred at 1.81 mm/s and 2.27 mm/s (Fig. 3*b*). Following previous Mössbauer work on (Fe, $Mn)_3(PO_4)_2$ solid solutions (Nord and Ericsson, 1982), the component with a QS = 1.81 mm/s (relative area of 54%) is assigned to Fe^{2+} at the *M*2 site and that with a QS = 2.27 mm/s (relative area = 9%) to Fe^{2+} at the *M*3 site. Thus, in the beusite-(Ca) studied, 86% of Fe^{2+} occurs at the *M*2 site and 14% at the *M*3 site. This is in accord with

TABLE 5. Atom coordinates and anisotropic displacement parameters for beusite-(Ca).

Atom	x	y	z	U^{11}	U^{22}	U^{33}	U^{23}	U^{13}	U^{12}	U_{eq}
M(1)	0.94894(3)	0.12351(2)	0.82833(4)	0.01427(13)	0.01039(13)	0.01330(13)	−0.00136(8)	0.00017(9)	0.00011(8)	0.0129(1)
M(2)	0.71246(2)	0.07833(2)	0.32707(3)	0.01367(11)	0.02039(12)	0.00700(10)	0.00024(6)	0.00153(7)	0.00437(7)	0.0137(1)
M(3)	0.35905(3)	0.19028(2)	0.13246(3)	0.01322(11)	0.01207(11)	0.01001(11)	0.00025(6)	0.00141(7)	0.00250(6)	0.0118(1)
P(1)	0.09269(4)	0.13378(3)	0.39637(5)	0.00773(14)	0.00825(14)	0.00829(15)	−0.00009(10)	0.00169(11)	−0.00055(10)	0.0080(1)
P(2)	0.60018(4)	0.08968(3)	0.80755(5)	0.00756(14)	0.00931(15)	0.00675(14)	0.00004(10)	0.00175(11)	0.00054(10)	0.0078(1)
O(1)	0.08211(12)	0.07072(9)	0.17752(16)	0.0169(5)	0.0115(4)	0.0100(4)	−0.0024(3)	0.0019(4)	0.0005(3)	0.0128(2)
O(2)	0.47152(11)	0.17524(9)	0.83172(16)	0.0113(4)	0.0143(4)	0.0119(4)	0.0014(3)	0.0036(3)	0.0048(3)	0.0123(2)
O(3)	0.93707(12)	0.18677(9)	0.42698(17)	0.0107(4)	0.0169(5)	0.0151(5)	−0.0005(4)	0.0043(4)	0.0037(3)	0.0140(2)
O(4)	0.68584(11)	0.12832(8)	0.62280(16)	0.0123(4)	0.0150(5)	0.0085(4)	0.0004(3)	0.0043(3)	−0.0017(3)	0.0117(2)
O(5)	0.20745(12)	0.23269(9)	0.38288(17)	0.0168(5)	0.0157(5)	0.0117(4)	−0.0007(4)	0.0037(4)	−0.0092(4)	0.0146(2)
O(6)	0.72454(11)	0.09121(9)	0.01365(16)	0.0091(4)	0.0177(5)	0.0074(4)	−0.0003(3)	0.0004(3)	−0.0001(3)	0.0115(2)
O(7)	0.14462(12)	0.05912(9)	0.59685(16)	0.0164(4)	0.0117(4)	0.0114(4)	0.0032(3)	0.0007(3)	0.0006(3)	0.0133(2)
O(8)	0.53394(11)	−0.03234(8)	0.76444(16)	0.0108(4)	0.0095(4)	0.0129(4)	−0.0000(3)	0.0014(3)	−0.0010(3)	0.0111(2)

https://doi.org/10.1180/mgm.2018.120 Published online by Cambridge University Press

TABLE 6. Selected interatomic distances (Å) in beusite-(Ca).

M(1)–O(1A)	2.293(1)	*M*(2)–O(3)	2.348(1)	*M*(3)–O(1)	2.863(1)
M(1)–O(1B)	2.364(1)	*M*(2)–O(4)	1.966(1)	*M*(3)–O(2A)	2.246(1)
M(1)–O(3)	2.571(1)	*M*(2)–O(6)	1.960(1)	*M*(3)–O(2B)	2.142(1)
M(1)–O(3B)	2.313(1)	*M*(2)–O(7)	2.052(1)	*M*(3)–O(5)	2.253(1)
M(1)–O(4)	2.456(1)	*M*(2)–O(8)	2.218(1)	*M*(3)–O(5B)	2.076(1)
M(1)–O(5)	2.808(1)	<*M*(2)–O>	2.109	*M*(3)–O(8)	2.128(1)
M(1)–O(6)	2.465(1)			<*M*(3)–O>	2.285
M(1)–O(7)	2.523(1)				
<*M*(1)–O>	2.474				
P(1)–O(1)	1.529(1)	*P*(2)–O(2)	1.538(1)		
P(1)–O(3)	1.543(1)	*P*(2)–O(4)	1.532(1)		
P(1)–O(5)	1.549(1)	*P*(2)–O(6)	1.539(1)		
P(1)–O(7)	1.524(1)	*P*(2)–O(8)	1.552(1)		
<*P*(1)–O>	1.536	<*P*(2)–O>	1.540		

the results of Nord and Ericsson (1982) that Fe^{2+} preferentially enters the [5]-coordinated *M*2 site.

Powder X-ray diffraction

Beusite-(Ca) is intimately intergrown with exsolved lamellae of triphylite and cannot be separated. Thus we collapsed the single-crystal data to produce an experimental diffraction pattern (for Cu*K*α) that simulates that of a powder pattern (in much the same way as a Gandolfi apparatus). The pattern is given Table 3.

Crystal structure

A single crystal (30 μm × 30 μm × 60 μm) was attached to a tapered glass fibre and mounted on a Bruker D8 three-circle diffractometer equipped with a rotating-anode generator (Mo*K*α X-radiation), multilayer optics and an APEX-II detector. In excess of a Ewald sphere of data was collected to 60°2θ using 4 s per 0.2° frame with a crystal-to-detector distance of 5 cm. Empirical absorption corrections (*SADABS*; Sheldrick, 2008) were applied and equivalent reflections were merged, resulting in 1852 unique reflections. Unit-cell dimensions (Table 4) were obtained by least-squares refinement of the positions of 4083 reflections with $I > 10\sigma I$. In principle, three scattering species cannot be refined over three sites in a crystal structure (Hawthorne, 1983), and site assignment becomes more difficult where scattering species of similar atomic number (i.e. Fe and Mn) are involved. We dealt with this problem by: (1) freely refining site-scattering values at the three *M* sites; (2) assigning all Ca to *M*(1) on the basis of the observed bond-lengths and the resulting bond-valence sums; and (3) assigning Fe to *M*(2) and M(3) on the basis of the Mössbauer results (Table 2). The structure was refined to an R_1 index of 1.55%. Miscellaneous information concerning structure solution and refinement is listed in Table 4. Atom positions and equivalent isotropic-displacement parameters are given in Table 5, selected interatomic distances in Table 6, refined

TABLE 7. Site-scattering values (epfu) and site populations (apfu) in beusite-(Ca).

Site	Site scattering	[CN] <*M*–O> Å	Site populations	Calculated site-scattering
M(1)	21.56(4)	[8] 2.474	0.94 Ca + 0.06 Mn^{2+}	20.30
M(2)	25.93(4)	[5] 2.109	0.79 Fe^{2+} + 0.21 Mn^{2+}	25.79
M(3)	25.64(4)	[6] 2.285	0.13 Fe^{2+} + 0.87 Mn^{2+}	25.13

epfu – electrons per formula unit; apfu – atoms per formula unit; [CN] – coordination number.

https://doi.org/10.1180/mgm.2018.120 Published online by Cambridge University Press

TABLE 8. Bond-valence* (valence units) table for beusite-(Ca).

	M(1)	*M*(2)	*M*(3)	*P*(1)	*P*(2)	Σ
O(1)	0.38		0.07	1.27		2.04
	0.32					
O(2)			0.29		1.24	1.91
			0.38			
O(3)	0.19	0.22		1.23		2.00
	0.36					
O(4)	0.26	0.52			1.26	2.04
O(5)	0.11		0.29	1.21		2.05
			0.44			
O(6)	0.25	0.53			1.24	2.02
O(7)	0.22	0.43		1.29		1.94
O(8)		0.29	0.39		1.20	1.88
Σ	2.09	1.99	1.86	4.99	4.94	

*Calculated from the parameters of Gagné and Hawthorne (2015).

site-scattering values (Hawthorne *et al.*, 1995) in Table 7, and a bond-valence calculation is shown in Table 8. Observed and calculated structure-factors and a crystallographic information file have been deposited with the Principal Editor of *Mineralogical Magazine* and are available as Supplementary material (see below).

Beusite-(Ca) is isostructural with the rest of the minerals of the graftonite group. As indicated in Table 7, Mn^{2+} is strongly ordered at the [6]-coordinated *M*(3) site, and a minor amount of Mn^{2+} occurs at *M*(1). Note that the ordering of Mn^{2+} and Fe^{2+} over the *M*(2) and *M*(3) sites is not part of the classification criteria for this group as it requires crystal-structure refinement and Mössbauer spectroscopy to determine the site populations of *M*(2) and *M*(3) (Hawthorne and Pieczka, 2018). With regard to classification, the formula is written as $(Ca_{0.94}Mn_{1.13}Fe_{0.92})_{\Sigma 3}(PO_4)_2$ which gives the ideal formula: $CaMn_2(PO_4)_2$. The position of the holotype composition of beusite-(Ca) in the classification scheme for the minerals of the graftonite group (Hawthorne and Pieczka, 2018) is shown in Fig. 4.

Origin

Beusite-(Ca) is a primary phase in a beryl–columbite–phosphate rare-element pegmatite, and formed during crystallization of the inner intermediate-zone and core of the pegmatite. Beusite-(Ca) is commonly intergrown with triphylite–lithiophilite and is thought to result from exsolution from a high-temperature (Li,Ca)-rich graftonite-like parent phase. The beusite-(Ca)–triphylite intergrowths are in sharp contact with blocky metasomatically altered pink microcline, and incipient Na-metasomatism is indicated by the presence of a small patch of alluaudite-group minerals near the intergrowths of beusite-(Ca) and triphylite. Minor ferrisicklerite is present as a weathering product of triphylite.

Acknowledgements

This work was supported by a Discovery grant from the Natural Sciences and Engineering Research

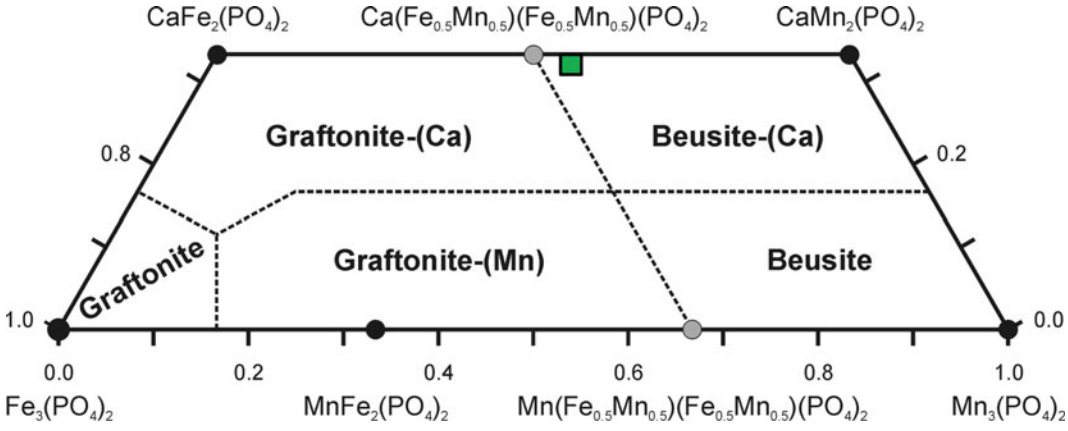

FIG. 4. The chemical composition of holotype beusite-(Ca) (green square, mean of 10 analyses) using the classification scheme of Hawthorne and Pieczka (2018).

https://doi.org/10.1180/mgm.2018.120 Published online by Cambridge University Press

Council of Canada and by grants from the Canada Foundation for Innovation to FCH. AP was supported by the AGH UST grant 11.11.140.319, and AW by the National Science Centre (Poland) grant 2015/17/N/ST10/02666.

We thank Fernando Colombo, Pete Leverett and Frédéric Hatert for their comments on this paper.

Supplementary material

To view supplementary material for this article, please visit https://doi.org/10.1180/mgm.2018.120

References

Bartelmehs, K.L., Bloss, F.D., Downs, R.T. and Birch, J. B. (1992) Excalibr II. *Zeitschrift für Kristallographie*, **199**, 186–196.

Beus, A.A. (1950) Magniophilite and mangankoninckite, two new minerals from pegmatites. *Doklady Akademii Nauk SSSR*, **73**, 1267–1279.

Bild, R.W. (1974) New occurrences of phosphates in iron meteorites. *Contributions to Mineralogy and Petrology*, **45**, 91–98.

Calvo, C. (1968) The crystal structure of graftonite. *American Mineralogist*, **53**, 742–750.

Černý, P. (1989) Exploration strategy and methods for pegmatite deposits of tantalum. Pp. 274–302 in: *Lanthanides, Tantalum and Niobium* (P. Möller, P. Černý and F. Saupe, editors). Springer-Verlag, New York.

Černy, P., Selway, J.B., Ercit, T.S., Breaks, F.W., Anderson, A.J. and Anderson, S.D. (1998) Graftonite-beusite in granitic pegmatites of the Superior Province: A study in contrasts. *The Canadian Mineralogist*, **36**, 367–376.

Ercit, T.S., Tait, K., Cooper, M.A., Abdu, Y., Ball, N.A., Anderson, A.J., Černý, P., Hawthorne, F.C. and Galliski, M. (2010) Manitobaite, $Na_{16}Mn^{2+}_{25}Al_8(PO_4)_{30}$, a new phosphate mineral from Cross Lake, Manitoba, Canada. *The Canadian Mineralogist*, **48**, 1455–1463.

Fransolet, A.-M., Keller, P. and Fontan, F. (1986) The phosphate mineral associations of the Tsaobismund pegmatite, Namibia. *Contributions to Mineralogy and Petrology*, **92**, 502–517.

Gagné, O. and Hawthorne, F.C. (2015) Comprehensive derivation of bond-valence parameters for ion pairs involving oxygen. *Acta Crystallographica*, **B71**, 562–578.

Galliski, M.A., Oyarzábal, J.C., Márquez-Zavalía, M.F. and Chapman, R. (2009) The association qingheiite-beusite-lithiophilite in the Santa Ana pegmatite, San Luis, Argentina. *The Canadian Mineralogist*, **47**, 1213–1223.

Guastoni, A., Nestola, F., Mazzoleni, G. and Vignola, P. (2007) Mn-rich graftonite, ferrisicklerite, stanĕkite and Mn-rich vivianite in a granitic pegmatite at Soè Valley, central Alps, Italy. *Mineralogical Magazine*, **71**, 579–585.

Hålenius, U.F., Hatert, F.M., Pasero, M. and Mills, S.J. (2017) CNMNC Newsletter No. 36, April 2017, *Mineralogical Magazine*, **81**, 403–409.

Hawthorne, F.C. (1983) Quantitative characterization of site-occupancies in minerals. *American Mineralogist*, **68**, 287–306.

Hawthorne, F.C. (1998) Structure and chemistry of phosphate minerals. *Mineralogical Magazine*, **62**, 141–164.

Hawthorne, F.C. and Pieczka, A. (2018) Classification of the minerals of the graftonite group. *Mineralogical Magazine*, **82**, 1301–1306.

Hawthorne, F.C., Ungaretti, L. and Oberti, R. (1995) Site populations in minerals: terminology and presentation of results of crystal-structure refinement. *The Canadian Mineralogist*, 33, 907–911.

Huminicki, D.M.C. and Hawthorne, F.C. (2002) The crystal chemistry of phosphate minerals. Pp. 123–253 in: *Phosphates – Geochemical, Geobiological and Materials Importance* (M.L. Kohn, J. Rakovan and J. M. Hughes, editors). Reviews in Mineralogy & Geochemistry, **48**. Mineralogical Society of America and the Geochemical Society, Washington, DC.

Hurlbut, C.S., Jr. and Aristarain, L.F. (1968) Beusite, a new mineral from Argentina, and the graftonite–beusite series. *American Mineralogist*, **53**, 1799–1814.

Nord, A.G. and Ericsson, T. (1982) The cation distribution in synthetic $(Fe,Mn)_3(PO_4)_2$ graftonite-type solid solutions. *American Mineralogist*, **67**, 826–832.

Olsen, E.J., Kracher, A., Davis, A.M., Steele, I.M., Hutcheon, I.D. and Bunch, T.E. (1999) The phosphates of IIIAB iron meteorites. *Meteorics and Planetary Science*, **34**, 285–300.

Penfield, S.L. (1900) On graftonite, a new mineral from Grafton, New Hampshire and its intergrowth with triphylite. *American Journal of Science*, **159**, 20–32.

Pieczka, A. (2007) Beusite and an unusual Mn-rich apatite from the Szklary granitic pegmatite, Lower Silesia, southwestern Poland. *The Canadian Mineralogist*, **45**, 901–914.

Pouchou, J.L. and Pichoir, F. (1985) 'PAP' ($\varphi\rho Z$) procedure for improved quantitative microanalysis. Pp. 104–106 in: *Microbeam Analysis* (J.T. Armstrong, editor). San Francisco Press, San Francisco, California, USA.

Rancourt, D.G. and Ping, J.Y. (1991) Voigt-based methods for arbitrary-shape static hyperfine parameter distributions in Mössbauer spectroscopy. *Nuclear Instruments and Methods in Physics Research*, **B58**, 85–97.

Sheldrick, G.M. (2008) A short history of SHELX. *Acta Crystallographica*, **A64**, 112–122.

Smeds, S.A., Uher, P., Černý, P., Wise, M.A., Gustafsson, L. and Penner, P. (1998) Graftonite – beusite in Sweden: primary phases, products of exsolution, and distribution in zoned populations of granitic pegmatites. *The Canadian Mineralogist*, **36**, 377–394.

Stalder, M. and Rozendaal, A. (2002) Graftonite in phosphatic iron formations associated with the mid-Proterozoic Gamsberg Zn-Pb deposit, Namaqua Province, South Africa. *Mineralogical Magazine*, **66**, 915–927.

Steele, I.M., Olsen, E., Pluth, J. and Davis, A.M. (1991) Occurrence and crystal structure of Ca-free beusite in the El Sampal IIIA iron meteorite. *American Mineralogist*, **76**, 1985–1989.

Tait, K.T., Hawthorne, F.C. and Wise, M.A. (2013) The crystal structure of the graftonite–beusite minerals. *The Canadian Mineralogist*, **51**, 653–662.

Vignola, P., Diella, V., Oppizzi, P., Tiepolo, M. and Weiss, S. (2008) Phosphate assemblages from the Brissago granitic pegmatite, western southern Alps, Switzerland. *The Canadian Mineralogist*, **46**, 635–650.

Wise, M.A. and Černý, P. (1990) Beusite-triphylite intergrowths from the Yellowknife pegmatite field, Northwest Territories. *The Canadian Mineralogist*, **28**, 133–139.

Wise, M.A., Hawthorne, F.C. and Černý, P. (1990) Crystal structure of a Ca-rich beusite from the Yellowknife pegmatite field, North West Territories. *The Canadian Mineralogist*, **28**, 141–146.

https://doi.org/10.1180/mgm.2018.120 Published online by Cambridge University Press